Analysis of the Source of Dynamic Interfacial Phenomena during Reaction between Metal Droplets and Slag

M.A. RHAMDHANI, K.S. COLEY, and G.A. BROOKS

The dynamic interfacial phenomena during high-temperature reaction between an Fe-Al alloy droplet and a $CaO-SiO_2-Al_2O_3$ slag were analyzed by evaluating the thermocapillary, solutocapillary, and electrocapillary effects. The magnitudes of these effects were determined using the local equilibrium model and utilizing kinetic data to determine local composition, temperature, and electrical potential. The electrocapillary effect was found to be dominant. It contributed approximately 85 pct of the maximum interfacial depression while the solutocapillarity contributed 15 pct. The thermocapillary effect was found to be negligible. In this work, the local gradient of interfacial tension along the interface due to the solutocapillary effect was estimated, *i.e.*, $\Delta\gamma_{m\text{-}s}$ = 274 to 440 mN/m over a 1- to 2-μm distance.

I. INTRODUCTION

DYNAMIC interfacial phenomena during reactions between liquid metal and liquid slag have been of interest to many investigators.[1–6] In the case of a liquid iron alloy droplet reacting with liquid slag, the phenomena include interfacial turbulence, a decrease in dynamic interfacial tension indicated by droplet flattening or spreading, and spontaneous emulsification where the droplet breaks into numerous droplets.[1–6] The term "dynamic" in dynamic interfacial tension is used to distinguish it from the value of equilibrium interfacial tension, although it may actually be a local equilibrium phenomenon. In fact, in the present work, dynamic interfacial tension has been analyzed in terms of local equilibrium. These phenomena occur without external forces being applied, have an important role in process metallurgy since they can increase the global rate significantly through the spontaneous increase of interfacial area, and enhance mass transport up to several orders.[7]

Previous Work on Dynamic Interfacial Phenomena

Kozakevitch *et al.*[1] were among the first to report the interfacial phenomena during reactions between iron alloy and slag. They conducted experiments in which liquid Fe-C-S droplets reacted with a blast furnace slag, $CaO-SiO_2-Al_2O_3$. They observed, from an X-ray photograph, a drastic lowering of dynamic interfacial tension and droplet shape changes during the desulfurization reaction followed by recovery of the droplet shape at the end of the reaction. Ooi *et al.*[2] confirmed these phenomena and showed that they also occur during the oxidation reactions of Fe-Al and Fe-Ti alloys with $CaO-Al_2O_3-SiO_2$ slag. In the case of reaction between Fe-Al alloys with $CaO-SiO_2-Al_2O_3$ slag, they suggested that droplet dynamic phenomena were due to the reduction reaction of silica in the slag by aluminum as follows:

$$\underline{Al} + \frac{3}{4}(SiO_2) = \frac{3}{4}\underline{Si} + \frac{1}{2}(Al_2O_3), \qquad \Delta H = -180{,}170\ \text{J} \quad [1]$$

where "_" indicates the element is dissolved in iron and "( )" indicates the compound is dissolved in slag.

More extensive experiments in this area were carried out by Riboud and Lucas[3] as they studied the influence of mass transfer upon interfacial phenomena. They found that the phenomena also occur in the reaction between oxidizing slags and most liquid iron systems containing oxidizable alloying elements, namely, Fe-Al, Fe-C-S, Fe-Ti, Fe-P, Fe-B, Fe-Cr, and Fe-Si alloys. They reported that the dynamic interfacial tension tends to zero when the oxygen flux is larger than 0.1 g atom $m^{-2}\ s^{-1}$. Riboud and Lucas also carried out microscopic observations in the vicinity of the interface of the quenched droplets and observed numerous metallic droplets with diameters ranging from 1 to 100 μm near the interface in the slag phase when the reaction is most intense. This spontaneous emulsification increases the interfacial area and can further affect the reaction rate.

Cramb and co-workers[4,5,6] continued the study of dynamic interfacial phenomena between liquid metal and slag. Sharan and Cramb[4] observed a lowering of interfacial tension during reaction between Fe-20 wt pct Ni-2.39 wt pct Al and $CaO-SiO_2-Al_2O_3$ slag at 1550 °C. In the case of Fe-Al alloy reacting with $CaO-SiO_2-Al_2O_3$ slag, Chung and Cramb[5,6] further investigated aluminum contents ranging from 0.25 to 3.3 wt pct and observed the droplet dynamic phenomena for aluminum contents as low as 0.25 wt pct. However, spontaneous emulsification and drastic lowering of dynamic interfacial tension were observed only for a system containing aluminum greater than 3 wt pct. Upon microscopic observation of the quenched samples, they found that at 5 minutes of reaction, one side of the droplet was deformed and optical microscopy observation showed entrapped slag in this region, suggesting that a local reaction may have occurred. Chung and Cramb also reported that the dynamic phenomena occur in reactions between liquid 321-stainless steels and ladle or mold slags.[6]

The phenomena also occur in systems other than liquid iron/steel and slag. Some investigators reported the phenomena in

M.A. RHAMDHANI, formerly Doctoral Student, Department of Materials Science and Engineering, McMaster University, Hamilton, ON, Canada, is Lecturer with the Department of Materials Science and Engineering, Institute of Technology Bandung, Bandung 40312, Indonesia. E-mail: rhamdhma@mcmaster.ca K.S. COLEY, Associate Professor, is with the Department of Materials Science and Engineering, McMaster University, Hamilton, ON, Canada, L8S 4L7. G.A. BROOKS, formerly Associate Professor, Department of Materials Science and Engineering, McMaster University, is Principal Research Scientist, CSIRO Minerals, Clayton South, VIC 3169, Australia.

Manuscript submitted June 2, 2004.

reactions between liquid copper and molten Na_2CO_3[8] or during reactions between Cu-Ni-Al alloy with Li_2O-Al_2O_3-SiO_2 slag.[9]

The phenomena described are well observed and recognized; however, they are not fully understood. They are usually associated with the presence of Marangoni flow/convection, a fluid flow driven by gradients of surface and interfacial tension. The gradient of surface or interfacial tension itself can be caused by three factors: a gradient of temperature (thermocapillary), a gradient of electrical potential (electrocapillary), and a gradient of surface-active solutes (solutocapillary). It may be that all of these factors are present and contribute to the Marangoni convection and interfacial phenomena. However, the dominant factor may differ from one system to another.

In the case of Fe-Al droplets reacting with CaO-SiO_2-Al_2O_3 slag, it is still not clear which effect is the dominant factor. Richardson[10] suggested that the build up of interfacial charges during rapid reaction, *i.e.*, the electrocapillary effect, may lead to the lowering of interfacial tension due to increased London forces or dipole interactions across the interface. Sharan and Cramb[4] suggested that the increase of oxygen potential at the interface due to reaction and mass transfer from the slag is responsible for the lowering of interfacial tension. This article will address this issue, *i.e.*, investigate the dominant source, by calculating the thermocapillary, solutocapillary, and electrocapillary effects from kinetic data.

II. EXPERIMENTAL

A. *Metal and Slag Preparation*

The experiments involve reactions between Fe-Al alloy droplets, containing 3.5, 4, 4.45, and 5 wt pct Al, with CaO-SiO_2-Al_2O_3 slag. Metal droplets of different weights, 1.7, 2.35, 2.5, and 3.45 g, were prepared by melting iron pieces 99.99 pct, vacuum remelted with ultra low oxygen content, and Al wire 99.9999 pct, in a small electric arc furnace in a high-purity argon atmosphere of 0.5 atm (O_2 and H_2O $<$5 ppm molar). The alloys remelted three times to ensure homogenization of the alloying element. The compositions of the metal droplets were reconfirmed using the inductively coupled plasma (ICP) analysis technique. The oxygen content was measured using the inert gas fusion technique and was found to be 50 ppm in average. This value, representing the total oxygen, did not change in a significant way with Al content. This low variation may reflect the fact that the starting Al content did not change greatly (3.5 to 5 wt pct) and the total oxygen is dominated by the oxygen contributed from the surface oxide layer of the droplet. Master slag of composition CaO-SiO_2-Al_2O_3 (40 pct:40 pct:20 pct in weight) was made by melting a mixed batch in the Pt crucible at 1600 °C. The amounts of slag used in each experiment were 50 and 140 g.

B. *Apparatus and Procedure*

A vertical tube furnace equipped with molybdenum disilicide heating elements along with gas and vacuum systems was used in this study, as shown in Figure 1. High-purity argon gas (O_2 and H_2O $<$5 ppm molar) was used during the experiments. The gas was passed through a gas purifying system consisting of columns filled with anhydrous $CaSO_4$ (drierite) and a furnace containing copper turnings running at 600 °C prior to entering the main furnace. This is to ensure that the atmosphere condition in the furnace has a very low moisture and oxygen content.

Slag was placed in a ZrO_2 crucible and suspended in the furnace using molybdenum wire. A silicone seal was used on the furnace end cap to seal and hold the wire. A solid iron alloy droplet was placed inside the alumina injection tube and suspended on the cap by using an Nd magnet (Figure 1). The diameter of the lower part of the tube was smaller than the diameter of the droplet. High-purity argon gas was then introduced into the furnace after the atmosphere inside had been purged by applying a vacuum pump. The furnace was then turned on and set to the desired temperature to melt the slag and held for 20 minutes to allow homogenization. The magnet was then removed so that the droplet would fall and be suspended at the bottom part of the alumina injection tube. When the temperature of the droplet exceeded its melting point, the droplet fell into the zirconia crucible. Preliminary experiments were conducted to determine the time required for the droplet to melt. It was found that the droplet fell into the crucible 2 minutes ($\pm$17 seconds) after the magnet had been removed. Therefore, the zero time for the reaction was set at 2 minutes after magnet removal.

After reaching a particular time, the bottom part of the furnace was opened by removing the clamp. The wire was cut from the top and the entire crucible containing molten slag and alloy droplet was quenched rapidly into water. The time from the zero time to the time when the crucible quenched into water was set to be the reaction time. The crucible containing quenched slag and metal was then crushed manually using a hammer. A gentle tap easily disintegrated the slag without deforming the metal droplets. The metal droplets were then collected for analysis by means of magnetic separation.

C. *Interfacial Area Measurements*

Interfacial areas, droplet shapes, sizes, and distributions were measured and determined for each reaction time, prior to chemical analysis of the droplets. The interfacial area was determined using two methods. The first method involved direct measurement of the dimensions of each metallic particle using a vernier caliper and a micrometer and also by employing image analysis. The second method used involved sticking small pieces of paper sized from 1×1 to 5×5 mm^2 to the surface of the droplets and calculating the total area of the paper required to cover the entire surface. The first method was used for droplets with a simple shape, while the latter method was used for more complicated shapes. For a simple shape such as a near spherical droplet, both methods gave the same value within $\pm$5 pct. Multiple experiments were carried out focusing on the periods before, during, and after maximum emulsification. A fair repeatability of the experiment in terms of interfacial area data was obtained within a maximum error of $\pm$10 pct.

D. *Chemical Analysis*

The quenched droplets were ground to remove the outer surface and then subjected to ultrasonic cleaning in acetone. The droplets were then dissolved in hydrochloric acid and the resulting solution was diluted. The chemical compositions,

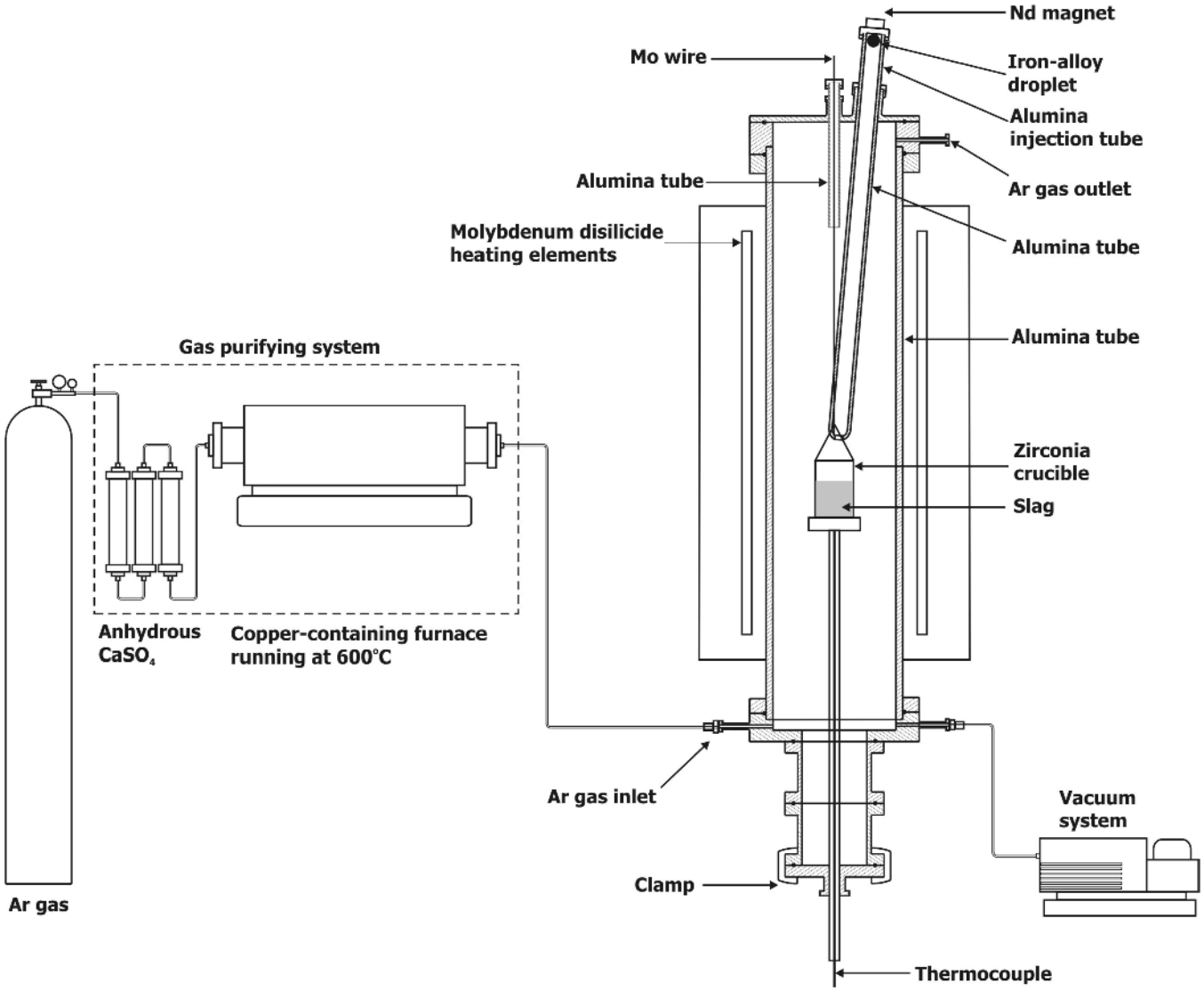

Fig. 1—Schematic of the experimental apparatus: tube furnace, vacuum, and gas purifying system used in the experiment.

Al and Si contents, were analyzed from the diluted solution against established standard solutions using an ICP emission spectrometer.

III. RESULTS AND DISCUSSION

A. *Interfacial Area, Droplet Number, and Shape Changes*

The interfacial area, droplet shapes, sizes, and distributions of the quenched droplets from each reaction time were examined. The recovered droplets during the progress of reaction showed a similar sequence of shape changes and droplet emulsification as those observed by previous investigators using X-ray radiography.[3,5] Both dynamic interfacial tension depression and spontaneous emulsification were observed in all four Fe-Al systems studied. For example, Figure 2 shows the droplet shape changes during the progress of the reaction in the case of reaction between 2.35 g Fe-4 wt pct Al and $CaO\text{-}SiO_2\text{-}Al_2O_3$ slag at 1650 °C. The changes in interfacial area and number of recovered droplets during the reaction are presented in Figures 3 and 4.

In the early stages of reaction, at 5 minutes, the recovered droplet has a flatter shape with a wavy and irregular interface indicating a decrease in the dynamic interfacial tension. The interfacial area was higher than that of the starting value. Although naked-eye observation suggests that only one droplet was recovered, microscopic observations at the interface revealed that, at 5 minutes, microscopic emulsification had occurred. These microscopic droplets were not taken into account in developing Figures 3 and 4 as they did not significantly change the overall interfacial area. Details of microscopic observations of the reacting interface have been described elsewhere.[11]

Numerous droplets, millimeter and micrometer in size, were recovered in the intermediate stage where the reaction was at its most intense, at 10 minutes. During this emulsification, the droplet disintegrated into a single droplet of a flatter shape, compared to the original, accompanied by numerous much smaller droplets, *i.e.*, more than 100 very small droplets with average diameter less than 1 mm. The main droplet had a very irregular interface resulting in a high interfacial area. The maximum increase of interfacial

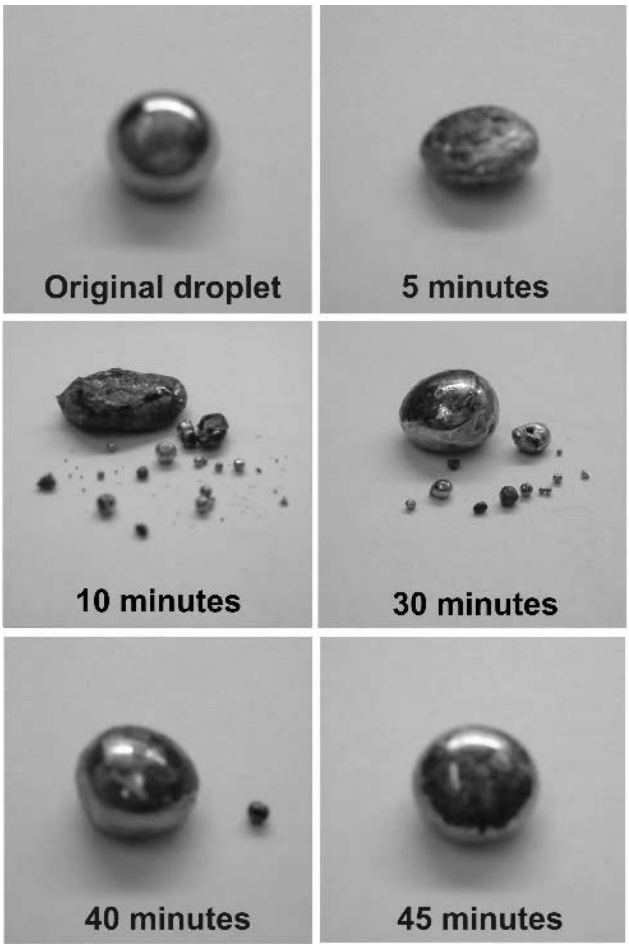

Fig. 2—Shape and number of droplets changes during reaction between 2.35 g Fe-4 wt pct Al and $CaO-SiO_2-Al_2O_3$ at 1650 °C.

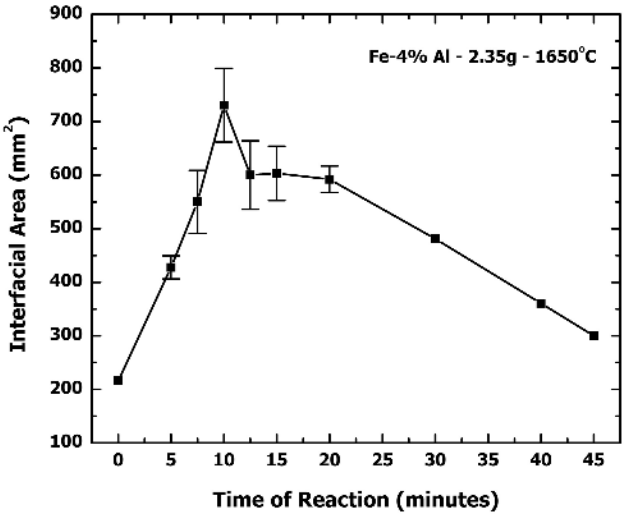

Fig. 3—Interfacial area changes during reaction between 2.35 g Fe-4 wt pct Al and $CaO-SiO_2-Al_2O_3$ at 1650 °C.

area during the reaction, about 375 pct of the initial value, was observed at this time of reaction.

As the reaction proceeded, the droplets recoalesced and the interfacial area and the number of droplets started to decrease.

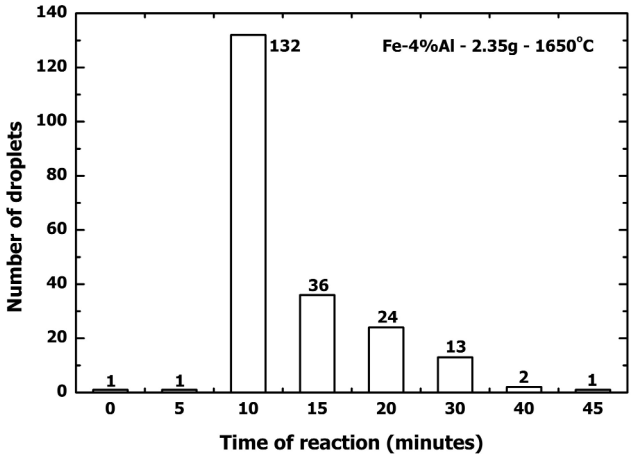

Fig. 4—Number of droplets recovered from the reaction between 2.35 g Fe-4 wt pct Al and $CaO-SiO_2-Al_2O_3$ at 1650 °C.

At 45 minutes of reaction, only a single droplet was recovered and it was nearly spherical and similar to the original droplet shape. However, it had a slightly higher volume (lower in density). This is associated with slag entrapment in the metal phase, as reported by previous investigators.[5,6]

The recovered droplets from other sets of experiments conducted under different experimental conditions showed a similar sequence to that described previously. The droplet flattened at the beginning of the reaction and immediately underwent spontaneous emulsification. The maximum increase of interfacial area was found to lie between 300 and 500 pct of the original value depending on the experimental conditions. The emulsified droplets then recoalesced as the reaction neared completion.

B. *Chemical Composition and Reaction Kinetics*

The metal droplets from each reaction time were analyzed and the chemical composition changes of the metal droplets during the reaction were determined. For example, Figures 5 and 6 show the change in Al and Si content for a reaction between 2.35 g Fe-5 wt pct Al and $CaO-SiO_2-Al_2O_3$ slag at 1650 °C and for 2.5 g Fe-4.45 wt pct Al at 1600 °C, respectively. These figures were developed from a composite of many experiments. As can be seen from the graphs, Al content in the metal droplets decreased while Si increased, suggesting that Reaction [1] took place during the process.

Kinetic analyses of the reaction were carried out using chemical composition data and interfacial area changes. It has been suggested from previous work that the kinetics follow a first-order relationship with respect to aluminum and the rate is controlled by mass transfer in the metal phase.[12,13] The details of the development of a transient treatment of kinetic data in the presence of spontaneous emulsification along with analyses and determination of the mass-transfer coefficients have been described elsewhere.[11,12,13]

C. *Thermocapillary Effect*

It has been suggested[2,3] that droplet dynamic phenomena were due to the reduction reaction of silica in the slag by aluminum, *i.e.*, Reaction [1]. The reaction is exothermic in nature and if the droplet is assumed to be thermally isolated, the

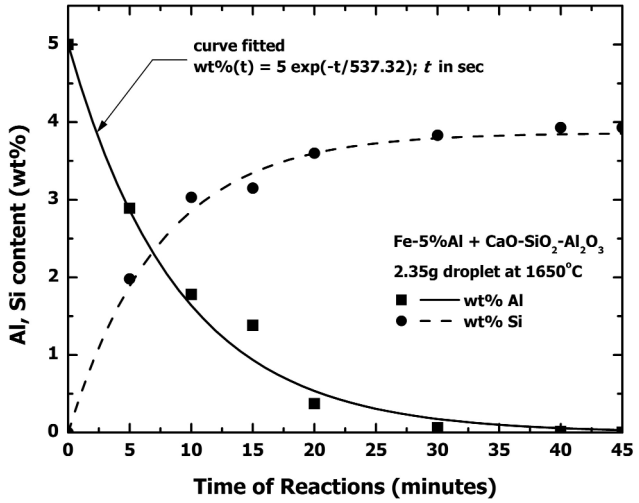

Fig. 5—The change of aluminum and silicon content of the 2.35 g Fe-5 wt pct Al droplet during reaction with $CaO\text{-}SiO_2\text{-}Al_2O_3$ slag at 1650 °C.

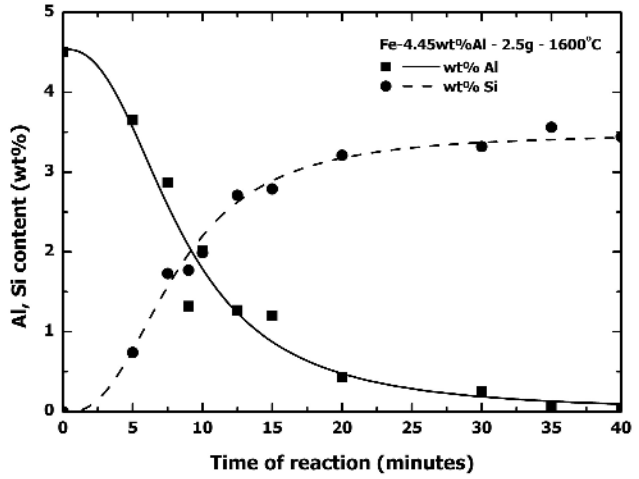

Fig. 6—The change in aluminum and silicon contents during a reaction between 2.5 g Fe-4.45 wt pct Al alloy droplet with $CaO\text{-}SiO_2\text{-}Al_2O_3$ slag at 1600 °C.

amount of heat generated can lead to an increase of temperature of 2.35 g Fe-5 wt pct Al sample by 414 °C. In actuality, the heat generated by the reaction is given off over time and the increase in the temperature will be much less than 414 °C. It is important to know the time scale over which the heat will dissipate and the temperature increase of the system during the reaction to understand their contribution to Marangoni convection and interfacial phenomena.

A simple heat-transfer model was developed. For a first approximation, the radiation effects were neglected. This assumption will provide a conservative estimate of the heat transfer, which will give an overestimate of the thermocapillary effect. Further, it was assumed that the droplet is spatially isothermal. The energy balance relates the rate of heat generated from the chemical reaction to the rate of heat loss (heat for increasing the droplet temperature and heat released to the slag through convection). Thus, the heat balance can be written as

$$\Delta H_R \cdot R(t) = n \cdot C_p \cdot \frac{dT}{dt} + h \cdot A \cdot (T - T_0) \qquad [2]$$

where ΔH_R is the heat of reaction (J/mol), $R(t)$ is the rate of reaction (mol/s), n is concentration (mol), C_p is the molar heat capacity (J/mol K), T is the temperature, h is the convection heat-transfer coefficient (W/m^2 K), and A is the droplet interface area (m^2).

Defining the temperature difference, $\theta = T - T_0$, and recognizing that $d\theta = dT$, Eq. [2] can be rearranged into

$$\frac{d\theta}{dt} + \frac{hA}{nC_p}\theta = \frac{\Delta H_R}{nC_p} R(t) \qquad [3]$$

Equation [3] is a linear differential equation and can be solved by calculating an exponential factor of $\int \exp(hA/nC_p)\cdot dt$ and writing

$$\frac{d}{dt}\left[\theta \cdot e^{\frac{hA}{nC_p}t}\right] = \frac{\Delta H_R}{nC_p} R(t) \cdot e^{\frac{hA}{nC_p}t} \qquad [4]$$

or

$$\theta \cdot e^{\frac{hA}{nC_p}t} = \frac{\Delta H_R}{nC_p}\int R(t)\, e^{\frac{hA}{nC_p}t}\, dt \qquad [5]$$

Equation [5] is obtained by assuming that C_p and A are constant. The assumption of constant interfacial area would give an overestimate of the thermocapillary effect. In this calculation, initial droplet interfacial area is used for the value of A. The $R(t)$ function is sought to solve Eq. [5]. The $R(t)$ function is determined from the change of composition during reaction. Figure 5 shows the change in aluminum content of the droplets during the reaction between Fe-5 wt pct Al alloy and $CaO\text{-}SiO_2\text{-}Al_2O_3$ slag at 1650 °C. The Al changes were curve fitted and represented by an exponential decay equation shown in the graph. Thus,

$$R(t) = \frac{dC(t)}{dt} = \frac{d}{dt}\left[W(t)\cdot\frac{2.35\text{g}}{27}\right] = -8.1\cdot 10^{-6}\, e^{-(t/537.32)} \qquad [6]$$

where

$$W(t) = 5e^{-(t/537.32)} \qquad [7]$$

that is the change in Al content in weight percent. Substituting the $R(t)$ function into Eq. [5],

$$\theta \cdot e^{\frac{hA}{nC_p}t} = -\frac{8.1\cdot 10^{-6}\cdot \Delta H_R}{nC_p}\int e^{\left(\frac{hA}{nC_p}-\frac{1}{537.32}\right)t} dt \qquad [8]$$

By integrating and rearranging Eq. [8], the following is obtained:

$$\theta = -\frac{8.1\cdot 10^{-6}\cdot \Delta H_R}{hA - (nC_p/537.32)}\cdot e^{-(1/537.32)t} + G\cdot e^{-(hA/nC_p)t} \qquad [9]$$

By applying the boundary condition $\theta(0) = 0$ or $\theta(\infty) = 0$, it follows that

$$G = \frac{8.1\cdot 10^{-6}\cdot \Delta H_R}{hA - (nC_p/537.32)} \qquad [10]$$

By substituting G into Eq. [10], the equation becomes

$$\theta = \Delta T = \frac{8.1\cdot 10^{-6}\cdot \Delta H_R}{hA - (nC_p/537.32)}\cdot\left[\frac{1}{e^{(hA/nC_p)t}} - \frac{1}{e^{(1/537.32)t}}\right] \qquad [11]$$

Table I. Properties of Liquid Iron, Liquid Slag, and Parameter Values

2.35 g–Fe-5 wt pct Al droplet ($D \sim 8$ mm) in $CaO\text{-}SiO_2\text{-}Al_2O_3$ slag at 1650 °C	
Heat of reaction, ΔH_R	−180, 170J/mol Al
Molar heat capacity, C_p	41.8 J/mol K
Interface area, A	2.01×10^{-4} m^2
Molar Fe, n	0.0448 mol
Convection heat-transfer coefficient of slag, h	250, 1250, and 2500 W/m^2 K
Thermal conductivity of liquid droplet, $k_{droplet}$	33 W/mK
Thermal conductivity of liquid slag, k_{slag}	1 W/mK
Bi (Biot number)	$hR/3k_{droplet}$
Nu (Nusselt number)	hD/k_{slag}
Ra (Rayleigh number)	$\mathrm{GrPr} = g\beta\Delta TL_c^3/\nu\alpha$

The increase of temperature during the reaction can then be evaluated from Eq. [11]. In this analysis, it was assumed that the slag temperature does not change during the reaction due to the large slag-to-metal ratio.

X-ray observations by Chung and Cramb[5,6] showed a displacement of smaller droplets and suggested some fluid flow in the slag phase, which is induced convectively by motion at the slag-metal interface or by natural convection in the slag. In our calculations, it is assumed that natural convection dominates the heat transfer from the droplet. The convective heat-transfer coefficient of a natural convection around sphere can be evaluated using the following relation:[14]

$$\mathrm{Nu} = 2 + 0.45\,(\mathrm{Ra})^{0.25} \qquad [12]$$

where Nu and Ra are the Nusselt and Rayleigh numbers, respectively. For laminar natural convection, the value of Ra is around 10^5. Taking the value of $\mathrm{Ra} = 10^5$, one will obtain the convective heat-transfer coefficient $h = 1250$ W/m^2 K, which corresponds to the value of Nu = 10. The Biot number, Bi, for this case is equal to 0.05, which justifies the assumption of a spatially isothermal droplet. A value of $h = 2500$ W/m^2 K is the critical value in which the Biot number, Bi, equals 0.1.

By substituting the parameters from Table I into Eq. [11], the increase of temperature during reaction can be determined. The changes of the temperature for various values of h are shown in Figure 7(a). It can be seen that the maximum increase of temperature is less than 6 K. For a limiting value of Nu = 2 or $h = 250$ W/m^2 K, in the absence of any convection, the maximum increase of temperature is 23.8 K (or °C).

The effect of temperature on the change of interfacial tension can then be evaluated. The surface and interfacial tension of most liquids decreases with increasing temperature. The variation usually follows a linear relation with a negative value of $(d\gamma/dT)$. The observed values of the temperature coefficient of surface tension of liquid iron, $(d\gamma_m/dT)$, lie between −0.02 and −0.5 mN/mK.[15] In the case of an Fe-C alloy in $CaO\text{-}SiO_2\text{-}Al_2O_3$ slag, the value of $(d\gamma_{m\text{-}s}/dT)$ is −1.48 mN/mK.[16] Assuming the similar $d\gamma_{m\text{-}s}/dT$ applies for an Fe-Al alloy, thus for a value of $h = 1250$ W/m^2 K, the interfacial tension depression, $\Delta\gamma_{m-s}$, will be −1.48 mN/mK × 6 K = −8.88 mN/m, as shown in Figure 7(b). This magnitude is very small compared to the original interfacial tension (about 1300 mN/m at 1650 °C). It corresponds to the change of interfacial tension of only 0.7 pct. For a limiting value of Nu = 2 ($h = 250$ W/m^2 K), the change of interfacial tension is only 2.7 pct.

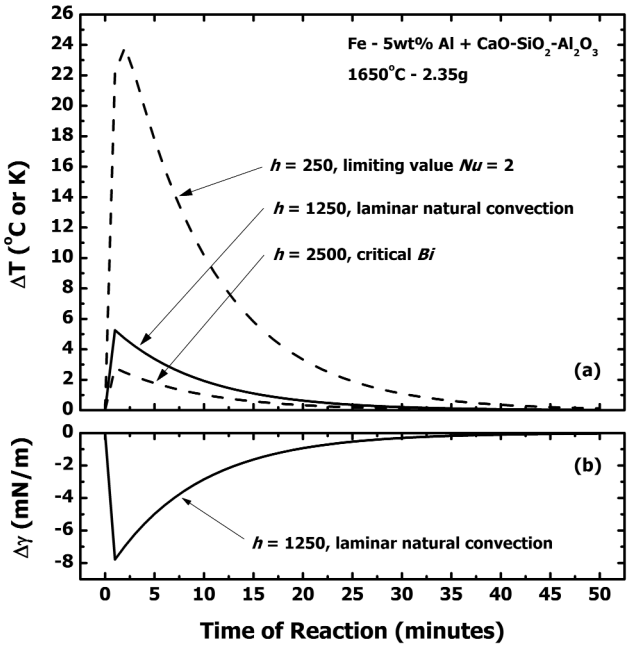

Fig. 7—(*a*) The increase of temperature during the reaction between 2.35 g-Fe-5 wt pct Al droplet and $CaO\text{-}SiO_2\text{-}Al_2O_3$ slag at 1650 °C for various values of heat-transfer coefficient, h. (*b*) The decrease of interfacial tension due to thermocapillary effect for the case of laminar natural convection.

The same approach can be applied for the case of a 2.5 g Fe-4.45 wt pct Al droplet reacting with the slag at 1600 °C. The maximum increase of temperature for this system was found to be 4.2 K, which corresponds to an interfacial tension change of 0.5 pct, as shown in Figures 8(a) and (b). These values may be considered negligible relative to the electrocapillary and solutocapillary effects discussed subsequently. Although the reaction is exothermic, the rate of heat accumulation is less then the rate of heat release. The model presented gives an overestimate temperature increase during the reaction because radiation was neglected. The actual temperature increase is likely to be lower than that calculated using the model. The authors did not consider it worthwhile to develop a more detailed heat-transfer model, because to consider radiation would merely render it even more negligible.

D. *Solutocapillary Effect*

In the case of reaction between Fe-Al alloy and $CaO\text{-}SiO_2\text{-}Al_2O_3$ slag, oxygen adsorption may occur. Oxygen may preferentially reside along the interface as opposed to the bulk due to its surface-active nature. This may significantly decrease the interfacial tension between the metal and the slag.

The effect of surface-active elements on the surface and interfacial tension of liquids can be described by the Szyszkowski[17] equation, *i.e.*, combination of the Gibbs and Langmuir adsorption isotherm equations. The application of this equation to liquid metals was first demonstrated by Belton.[18] The equation is written as

$$\gamma_0 - \gamma = \mathrm{R_g}\,T\,\Gamma_i^0\,\ln(1 + Ka_i) \qquad [13]$$

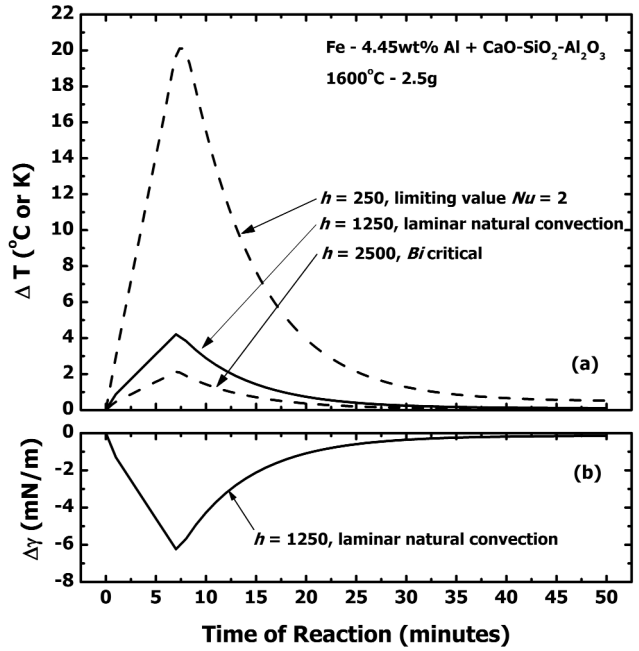

Fig. 8—(*a*) The increase of temperature during the reaction between 2.5 g-Fe-4.45 wt pct Al droplet and CaO-SiO_2-Al_2O_3 slag at 1600 °C for various values of heat-transfer coefficient, *h*. (*b*) The decrease of interfacial tension due to thermocapillary effect for the case of laminar natural convection.

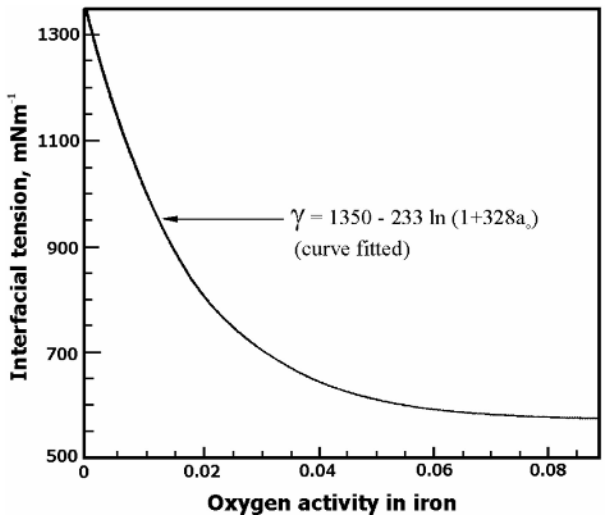

Fig. 9—The effect of oxygen activity on the interfacial tension between liquid iron and CaO-SiO_2-Al_2O_3 slag at 1600 °C, from Gaye *et al.*[20]

where $\gamma_o - \gamma$ is the surface/interfacial tension depression, R_g is the gas constant, T is the absolute temperature, Γ_i^0 is the saturation excess concentration of surface-active elements at the interface, K is the adsorption equilibrium constant, and a_i is the activity of surface-active elements. The application of Eq. [13] in explaining the effect of oxygen and sulfur on the interfacial tension between liquid iron and slag has been demonstrated by many investigators, as described in the work of Sun *et al.*[19]

The effect of oxygen on the interfacial tension between liquid iron and CaO-SiO_2-Al_2O_3 slag at 1600 °C, by means of the curve fitting of data from Gaye *et al.*,[20] can be written as

$$\gamma_{m-s} = 1350 - 233 \ln (1 + 328 a_O), \text{ mN/m} \qquad [14]$$

Figure 9 shows the decrease of interfacial tension as a function of oxygen activity in the case of liquid iron and CaO-SiO_2-Al_2O_3 slag at 1600 °C.[20] It can be seen that oxygen can decrease the interfacial tension from about 1350 mN/m to 550 mN/m, or about 60 pct.

The issue of oxygen in high-temperature reactions is complicated and not fully understood. For example, in an Fe-Al alloy reacting with a CaO-SiO_2-Al_2O_3 slag, mass transfer and adsorption of oxygen occur simultaneously and the fact that oxygen takes part in the reaction makes the matter more complicated. The oxygen is present in two forms, *i.e.*, dissolved oxygen and oxygen bound in oxides. Dissolved oxygen present in the bulk of the droplet and adsorbed along the interface. Oxygen as oxides includes an entrapped CaO-SiO_2-Al_2O_3 slag, Al_2O_3 inclusions, and Fe_2O_3.

To understand better the effect of oxygen on the Marangoni flow and moreover on the interfacial phenomena in general, knowledge of how oxygen is distributed in the metal is vital. There has been significant work on oxygen in high-temperature systems in terms of adsorption study, for example, in determining the oxygen surface excess.[20,21,22] However, there is only limited work on the actual oxygen concentration distribution along the interface and toward the bulk. Measurement of bulk oxygen contents can be performed by employing inert gas fusion analysis. However, oxygen in the form of inclusions and entrapped slag contributes some complication in determining the actual bulk oxygen content.

In this work, the oxygen composition changes during the reaction were calculated numerically from the kinetic data, *i.e.*, composition changes in the droplets. It was assumed that the interfacial tension was in local equilibrium with the instantaneous interface metal chemistry, an assumption that is similar to the common assumption that equilibrium is achieved at interfaces for reacting systems under mass-transfer control.

During high levels of mass transfer, the oxygen activity in the layer immediately adjacent to the interface will be higher than the bulk oxygen activity. There is also a gradient in aluminum and silicon concentration with respect to the bulk, as schematically shown in Figure 10. Consequently, the region near the interface will have a depleted Al concentration resulting in an elevated local oxygen activity. It is this "near interface" oxygen activity that will provide the driving force for surface segregation and interfacial tension depression. Thus, this value should be used for calculation using Eq. [14]. It was further assumed in the calculation that the oxygen concentration is governed by the dissociation reaction of silica at the interface as follows:

$$(SiO_2) = \underline{Si}_{int} + 2\underline{O}_{int} \qquad [15]$$

The preceding assumptions will provide an overestimate of the solutocapillary effect because they will give maximum values of local equilibrium oxygen activities.

Mass transfer of aluminum and silicon through the boundary layer in the metal phase was considered and the following equations were written:

$$\frac{d \text{ pct Si}}{dt} = \frac{k_m^{Si} \cdot S(t)}{V_m} \left(\text{pct Si}^{int} - \text{pct Si}^{bulk}\right) = Z_{Si} \left(\text{pct Si}^{int} - \text{pct Si}^{bulk}\right) \qquad [16]$$

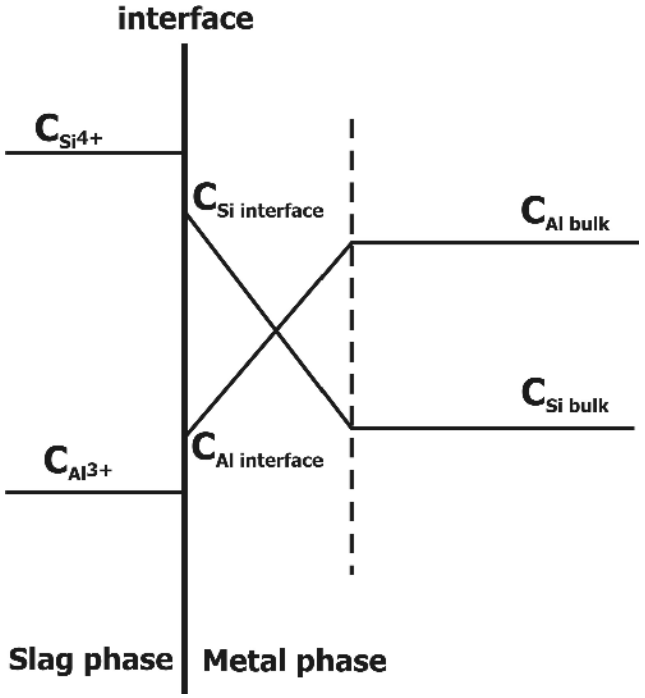

Fig. 10—Schematic of aluminum and silicon concentration gradients in the boundary layer during reaction controlled by mass transfer in the metal phase.

$$\frac{d\,\text{pct Al}}{dt} = \frac{k_m^{\text{Al}} \cdot S(t)}{V_m}\left(\text{pct Al}^{\text{bulk}} - \text{pct Al}^{\text{int}}\right) = -Z_{\text{Al}}\left(\text{pct Al}^{\text{bulk}} - \text{pct Al}^{\text{int}}\right) \quad [17]$$

If discrete changes are considered,

$$\frac{\left(\text{pct Si}_{t+1}^{\text{bulk}} - \text{pct Si}_t^{\text{bulk}}\right)}{t_{t+1} - t} = Z_{\text{Si}} \cdot \left(\text{pct Si}_t^{\text{int}} - \text{pct Si}_t^{\text{bulk}}\right) \quad [18]$$

$$\frac{\left(\text{pct Al}_{t+1}^{\text{bulk}} - \text{pct Al}_t^{\text{bulk}}\right)}{t_{t+1} - t} = -Z_{\text{Al}} \cdot \left(\text{pct Al}_t^{\text{bulk}} - \text{pct Al}_t^{\text{int}}\right) \quad [19]$$

where $Z_{\text{Si}} = k_m^{\text{Si}} \cdot S(t)/V_m$, $Z_{\text{Al}} = k_m^{\text{Al}} \cdot S(t)/V_m$, k_m^{Si} and k_m^{Al} are the mass-transfer coefficients of silicon and aluminum in the metal, $S(t)$ is the instantaneous interfacial area, and V_m is the volume of the metal phase. It has been suggested from previous work[12] that the kinetics of the reaction are controlled by mass transfer of aluminum in the metal phase. The mass-transfer coefficient of aluminum, k_m^{Al}, in the case of reaction between 2.5 g Fe-4.45 wt pct Al and CaO-SiO_2-Al_2O_3 slag at 1600 °C has been determined and found to be 1.5×10^{-6} m/s.[12] The value of the mass-transfer coefficient of silicon, k_m^{Si}, was estimated to be 1.25 times higher than the mass transfer of aluminum, k_m^{Al}, because the value of $D_{\text{Si}} \sim 1.25\ D_{\text{Al}}$[23] at 1600 °C. The silicon and aluminum concentrations at the interface during the reaction were then determined numerically from kinetic data and the results are shown in Figures 11(a) and (b), respectively. An example of calculations for determining these concentrations at the interface is presented in the Appendix.

The local equilibrium oxygen contents were determined using thermodynamic calculations and by considering the

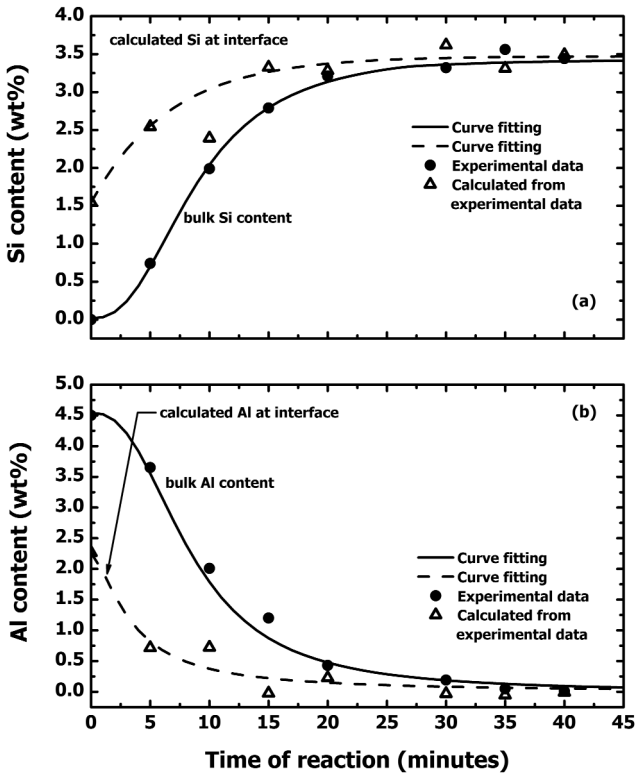

Fig. 11—The (*a*) silicon and (*b*) aluminum contents in the bulk (from experiments) and at the interface (calculated numerically) during reaction between 2.5 g Fe-4.45 pct wt Al droplet and CaO-SiO_2-Al_2O_3 slag at 1600 °C.

Table II. Interaction Coefficients Used in the Present Work[25,26]

i	*j*	e_i^j	$r_i^j (r_i^{i,j})$
Al	Al	0.043	−0.001
	O	−4.77	—
	Si	0.056	−0.0006
O	Al	−2.81	1.7
	O	−0.2	0
	Si	−0.131	0 (−0.0006*)
Si	Al	0.058	—
	O	−0.23	0 (0.00332*)
	Si	0.11	−0.0021

*The $r_i^{i,j}$ values are calculated from the second-order terms r_i^j using reciprocal relationships.[27]

activity of silica in the slag, $a_{(SiO_2)} = 0.25$[24] and the interface silicon and aluminum concentrations in the metal phase. The local activity of oxygen in the metal droplet was calculated from the activity coefficient of oxygen times the weight percent of oxygen (f_O [wt pct O]). The activity coefficients of oxygen, f_O, for each time in the reaction were determined by considering the instantaneous composition of Si, Al, and O and by considering the first- and second-order interaction coefficients. The interaction coefficients used in the calculation were taken from Deo and Boom[25] and Sigworth and Elliott,[26] as shown in Table II. An example of a calculation for determining the local equilibrium oxygen activity is presented in the Appendix.

Figure 12(a) shows the result of the calculation of local oxygen activity during the reaction. As the reaction started, the

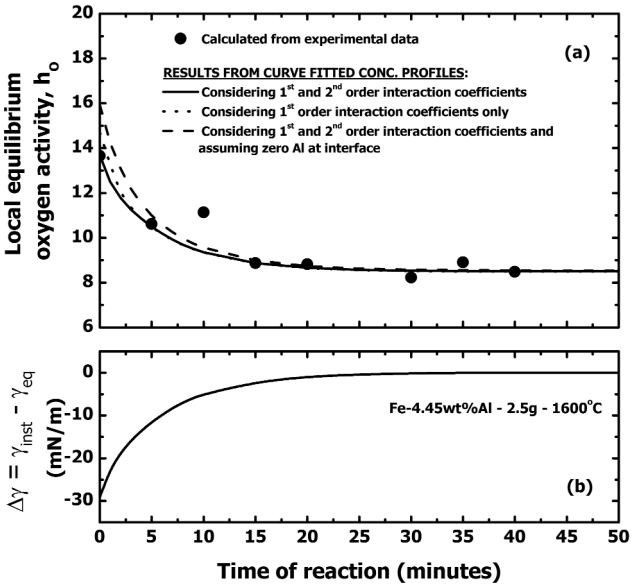

Fig. 12—(*a*) Calculated local equilibrium activity of oxygen and (*b*) interfacial tension depression due to solutocapillarity during reaction between 2.5 g Fe-4.45 pct wt Al droplet and CaO-SiO_2-Al_2O_3 slag at 1600 °C.

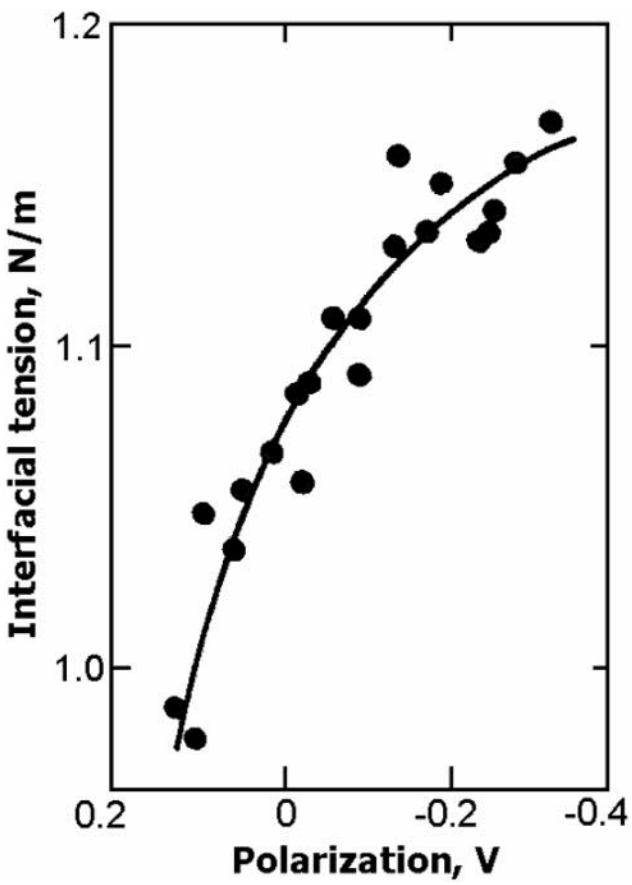

Fig. 13—The effect of applied electrical potential to the interfacial tension between liquid iron and liquid slag CaO-SiO_2-Al_2O_3 (40 wt pct-40 wt pct-20 wt pct) at 1550 °C, from Panfilov.[36]

oxygen activity decreased and leveled off to a value of oxygen activity in equilibrium with the final silicon and aluminum contents at the interface. The closed circles in the graph represent the result from calculation from experimental data points considering both first- and second-order interaction coefficients. The curves in Figure 12(a) show the results calculated from curve-fitted Si and Al concentration profiles, *i.e.*, dashed curves in Figures 11(a) and (b). The solid curve considers both first- and second-order interaction coefficients, while the dotted one considers only first-order interaction coefficients. There is a difference between these two curves during a period up to 4 minutes of reaction time. However, the difference is rather negligible, which suggests that the consideration of second-order coefficients is not essential. As has been mentioned earlier in this section, the region near the interface will have a depleted instantaneous Al concentration or may be down to zero if the transfer of Al to the interface is very slow. The dashed curve is the result from calculation assuming zero Al concentration at the interface, which gives the maximum possible levels of local oxygen activity during the reaction. It can be seen from the graph that this curve gives a higher oxygen activity compared to the other two up to 20 minutes of reaction. However, the difference is still in the range of experimental error. The three curves level off at the same level of oxygen activity toward the end of the reaction, *i.e.*, ~8.5 ppm.

The approach used in this work gives the maximum possible value of oxygen activities, hence the maximum effect of solutocapillarity. Supersaturation phenomenon during aluminum oxidation by silica has been reported by previous investigators.[28,29] The observed oxygen activity may reach a value of 4 times that of its equilibrium value (assuming constant a_{Al} with composition of 0.0017 to 0.41 wt pct Al). The supersaturation decreases with an increase of silicon and is not observed when the silicon content is higher than 0.5 wt pct.[29] In the system studied, the silicon content at the interface at the beginning of the reaction is calculated and found to be higher than 1.0 wt pct, as shown in Figure 11(a). This level of silicon increases as the reaction proceeds. Thus, supersaturation of oxygen activity near the interface in this case is not expected to occur.

The effect of oxygen on the interfacial tension of the droplet during the reaction then can be evaluated by using Eqs. [13] and [14]. Figure 12(b) shows the effect of oxygen (solutocapillary effect) on the interfacial tension depression during the reaction. It can be seen from the graph that originally the decrease of interfacial tension is −30 mN/m, and as the reaction proceeds, it decreases and levels off at zero. This magnitude is higher than that from the thermocapillary effect (~−6 mN/m).

E. *Electrocapillary Effect*

There is only limited work on electrocapillary behavior in high-temperature systems, especially in liquid iron in liquid CaO-SiO_2-Al_2O_3 slag.[30–36] Figure 13 shows an electrocapillary curve for liquid iron in liquid CaO-SiO_2-Al_2O_3.[36] Upon curve fitting of the data, the effect of applied electrical potential to the changes of interfacial tension can be written as

$$\gamma_{m-s} = 1165 - 694(\eta + 0.367)^2, \quad \text{mN/m} \qquad [20]$$

where η is the polarization in volts. The interface charge density is calculated by using the first derivation of Eq. [20]:

$$\frac{d\gamma_{m-s}}{d\eta} = -q = -1388\eta - 509.4, \quad \text{mN·V/m} \qquad [21]$$

Slag-metal reactions can be regarded as an electrochemical reaction that accompanies transfer of electrical charge. Thus, Reaction [1] can be written in terms of the following reactions:

$$\text{Anodic reaction:} \quad 4\underline{\text{Al}} = 4\text{Al}^{3+} + 12\text{e}^- \qquad [22]$$

$$\text{Cathodic reaction:} \quad 3\text{Si}^{4+} + 12\text{e}^- = 3\underline{\text{Si}} \qquad [23]$$

$$\text{Overall reaction:} \quad 4\underline{\text{Al}} + 3\text{Si}^{4+} = 4\text{Al}^{3+} + 3\underline{\text{Si}} \qquad [24]$$

It has been suggested from previous work[12] that the kinetics of the reaction are controlled by mass transfer of aluminum in the metal phase. Therefore, we can assume local equilibrium at the interface at all times and the Nersnt equation is applicable for calculating the instantaneous electrical potential difference across the interface, $\Delta\varphi(t)$, as follows:

$$\Delta\varphi(t) = \frac{R_g T}{12F} \ln\left[\left(\frac{a_{Al^{3+}}(t)}{a_{\underline{Al}_i}(t)}\right)^4 \left(\frac{a_{\underline{Si}_i}(t)}{a_{Si^{4+}}(t)}\right)^3\right] \qquad [25]$$

or in terms of concentration,

$$\Delta\varphi(t) = \frac{R_g T}{12F} \ln\left[\left(\frac{C_{Al^{3+}}(t)}{C_{\underline{Al}_i}(t)}\right)^4 \left(\frac{C_{\underline{Si}_i}(t)}{C_{Si^{4+}}(t)}\right)^3\right] \qquad [26]$$

where R_g is the gas constant; F is the Faraday's constant; T is temperature; and $a_{Al^{3+}}(t)$, $C_{Al^{3+}}(t)$, $a_{Si^{4+}}(t)$, $C_{Si^{4+}}(t)$, $a_{\underline{Al}_i}(t)$, $C_{\underline{Al}_i}(t)$, $a_{\underline{Si}_i}(t)$, and $C_{\underline{Si}_i}(t)$ are the instantaneous activities and concentrations of Al^{3+}, Si^{4+} in the slag and Al, Si in the metal, respectively. It was further assumed in the calculation that the concentrations (thus activities) of Al^{3+} and Si^{4+} in the slag are constant throughout the reaction, which is reasonable due to the large slag-to-metal volume ratio and that kinetic analysis of these results concluded that the overall rate is metal-phase mass-transfer controlled.[12]

The instantaneous polarization, $\eta(t)$, at the interface was calculated using the following equation:

$$\eta(t) = \Delta\varphi(t) - \Delta\varphi_{eq} \qquad [27]$$

where $\Delta\varphi_{eq}$ is the global equilibrium electrical potential difference, *i.e.*, at $t = \infty$. Thus,

$$\eta(t) = \Delta\varphi(t) - \Delta\varphi_{eq} = \frac{R_g T}{12F} \ln \frac{\left(a_{Al^{3+}}(t)\right)^4}{\left(a_{Si^{4+}}(t)\right)^3} \frac{\left(a_{Si^{4+}}(\infty)\right)^3}{\left(a_{Al^{3+}}(\infty)\right)^4} \times \frac{\left(a_{\underline{Sl}_i}(t)\right)^3}{\left(a_{\underline{Al}_i}(t)\right)^4} \frac{\left(a_{\underline{Al}_i}(\infty)\right)^4}{\left(a_{\underline{Si}_i}(\infty)\right)^3} \qquad [28]$$

Because $\left(a_{Al^{3+}}\right)^4 / \left(a_{Si^{4+}}\right)^3$ is constant with time,

$$\eta(t) = \frac{R_g T}{12F} \ln \frac{\left(a_{\underline{Si}_i}(t)\right)^3}{\left(a_{\underline{Al}_i}(t)\right)^4} \frac{\left(a_{\underline{Al}_i}(\infty)\right)^4}{\left(a_{\underline{Sl}_i}(\infty)\right)^3} \qquad [29]$$

Therefore, the shape of the polarization curve will only be affected by the activities of Al and Si at the interface in the metal side.

By considering that $\eta(\infty) = 0$, the polarization profile was developed. The kinetics information of Al and Si at the interface in the metal phase was used for the calculation, *i.e.*, dashed curves in Figures 11(a) and (b). Figure 14(a) shows the change in the polarization during the reaction between 2.5 g Fe-4.45 wt pct Al droplet with CaO-SiO_2-Al_2O_3 slag.

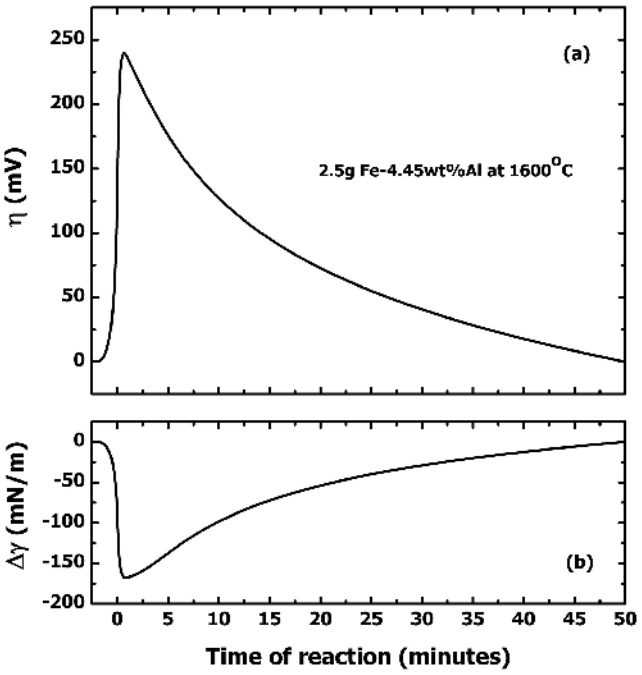

Fig. 14—(*a*) The change in polarization and (*b*) its effect on the interfacial tension during reaction between 2.5 g Fe-4.45 wt pct Al and CaO-SiO_2-Al_2O_3 slag at 1600 °C.

It can be seen from the graph that, as the reaction started, the polarization jumped to a level of 250 mV. The polarization decreased as the reaction proceeded and diminished as the rate of mass transfer slowed.

To calculate the effect of polarization on the interfacial tension depression, one needs to know the value of $d\gamma_{m\text{-}s}/d\eta$ and $\gamma_{m\text{-}s} = f(\eta)$. Assuming that Eqs. [20] and [21] applies in the system studied, the change in interfacial tension can be calculated. Figure 14(b) shows the interfacial tension change during the reaction due to the electrocapillary effect. It can be seen from the graph that as the reaction started, the interfacial tension rapidly dropped 175 mN/m. As the reaction proceeded, the depression of interfacial tension decreased to its equilibrium value at the end of the reaction. The magnitude of the interfacial tension depression from the electrocapillarity is much larger than that of the thermocapillary effect.

F. *Combined Effects*

The effects of temperature, electrical potential, and oxygen on the dynamic interfacial tension during the reaction between 2.5 g Fe-4.45 wt pct Al and CaO-SiO_2-Al_2O_3 slag were combined in one graph and shown in Figure 15. It can be seen from the graph that the effect of temperature is very small and can be neglected. The dominant effect in the system comes from the electrocapillary effect. Therefore, a mechanism involving the electrocapillary effect, as proposed by Richardson[10] to explain the lowering of interfacial tension, appears to be very significant. The contributions of solutocapillary and electrocapillary effects at the maximum interfacial tension depression are about 15 and 85 pct, respectively. Also shown in Figure 15 is the combined effect on the dynamic interfacial tension depression during the reaction.

Figure 16 shows the comparison between the calculated dynamic interfacial tension and the apparent interfacial tension

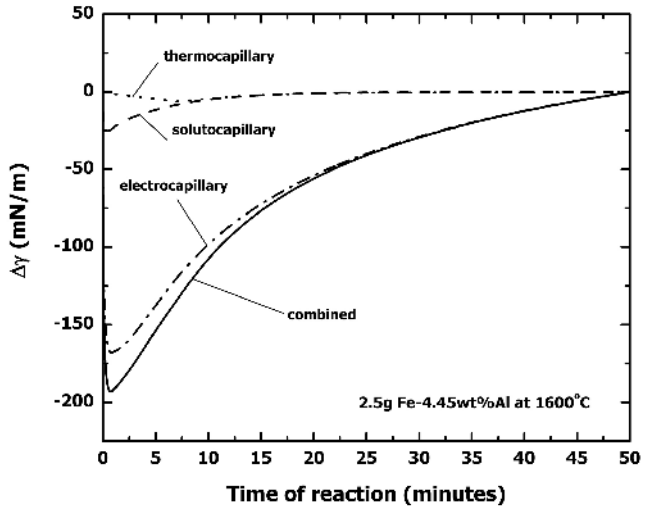

Fig. 15—Calculated interfacial tension depression due to thermocapillary, solutocapillary, and electrocapillary effects during reaction between 2.5 g Fe-4.45 pct wt Al droplet and $CaO\text{-}SiO_2\text{-}Al_2O_3$ slag at 1600 °C.

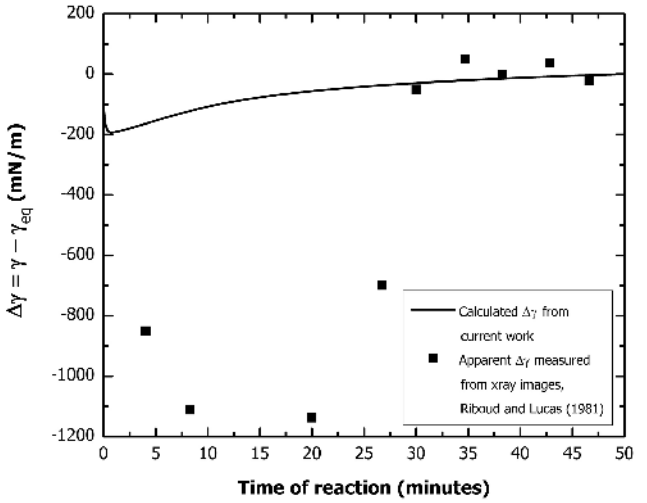

Fig. 16—Calculated and apparent interfacial tension measured from X-ray images from Riboud and Lucas[3] during reaction between 2.5 g Fe-4.45 pct wt Al droplet and $CaO\text{-}SiO_2\text{-}Al_2O_3$ slag at 1600 °C.

measured from X-ray photographs from Riboud and Lucas.[3] The calculation (solid curve) suggested that maximum depression occurs immediately after the reaction starts, while the measurement from Riboud and Lucas shows that maximum depression occurs after 7.5 minutes. The authors think that this is due to the lag of the response of droplet shape changes to the change of interfacial tension. The calculated value never reached an extent where the interfacial tension was extremely low (very high interfacial tension depression). Interfacial tension, whatever the value, will tend to minimize the interfacial area. Clearly, in reacting systems, including the current work, this area is not at a minimum. This suggests that reaction may lead to other forces that oppose the effect of interfacial tension and result in the flattening of the droplet. In fact, it appears that observations widely attributed to so-called "dynamic interfacial tension" are much more than just interfacial tension.

The discrepancies between the calculated and the observed values could also be partly related to our ability to measure interfacial tension of a rough reacting interface. It should be noted that Riboud and Lucas measured the interfacial tension by analyzing the X-ray photographs assuming a smooth shaped sessile droplet. Visual and scanning electron microscopy observations suggest that the interface is actually far from smooth, particularly when the depression is at a minimum. The droplets may also experience nonsymmetrical shape changes due to localized reactions, as has been reported by Chung and Cramb.[5] Spontaneous emulsification of both metal in slag and slag in metal can occur. This, especially slag emulsification, can change the main droplet density during the reaction and alter its shape and size. These facts will give large errors or even invalid measurements of the dynamic interfacial tension, especially during the period where spontaneous emulsification occurs.

The thermocapillary, solutocapillary, and electrocapillary effects on the dynamic interfacial tension of a reacting metal droplet have been analyzed by considering the reaction kinetic data. The temperature, electrical potential, and oxygen activity at the interface, or in the bulk immediately adjacent to it, change with respect to their bulk or equilibrium values due to reaction and mass transfer across the interface. Consequently, these combined effects lower the dynamic interfacial tension. However, the calculated value using the proposed local equilibrium model is not sufficient to explain the observed phenomenon. Whether this is a consequence of difficulties associated with experimental measurements or other physical chemical effects not yet considered has not been established and is worthy of further study.

G. *Microscopic Consideration*

Unlike the lowering of interfacial tension, a more localized and microscopic approach is required in analyzing the interfacial turbulence and spontaneous emulsification of the droplet during the reaction. As mentioned in Section I, these phenomena are usually associated with the Marangoni flow due to the concentration, thermal and electrical potential gradients along the interface. These gradients may be created by localized or nonuniform exothermic reaction at the interface and different rates of mass transfer along the interface. Evidence of nonuniform reaction in this system have been reported elsewhere.[5,37]

The mechanism for spontaneous emulsification is not fully understood and is still a subject of discussion. Chung and Cramb[6] proposed a mechanism for spontaneous emulsification through interfacial instability due to the Kelvin–Helmholtz instability. Since the reaction appears to initiate locally, it will cause both thermal and chemical variations at the interface. These will lead to variations of interfacial tension and give rise to Marangoni flow along the interface. Since the viscosities of metal and slag largely differ, the velocity of the motion of each phase parallel to the interface will be different. This will produce waves and perturbations along the interface. The perturbations can grow and form protrusions to both phases. Once these protrusions are formed, they tend to lower their interfacial area by becoming spherical and detaching themselves to form small emulsion droplets.

Based on the Kevin–Helmholtz model, Chung and Cramb[6] obtained the stability criteria of the interface. They suggested that the interface become unstable if the difference of velocity of metal and slag is greater than 25 cm/s. When the velocity difference exceeds 25 cm/s, waves can be generated with length 0.82 cm and velocity 18.4 cm/s. However, the observed wavelengths were much shorter than those obtained from the Kelvin–Helmholtz instability model,

i.e., ranging from 0.7 to 0.6 mm with majority of wavelength less than 1 μm. They claimed that the difference may be from an error in the estimated interfacial tension value used in the calculation or from a much greater driving flow resulting in low-wavelength interfacial perturbations.

Regardless of the mechanism for spontaneous emulsification, information about the local gradient of oxygen concentration, electrical potential, and temperature and also the length scale in which they are acting is vital for a comprehensive understanding of the interfacial phenomena. However, collection of these experimental data for high-temperature systems is inherently difficult and also limited by the instrument capabilities.

An attempt at quantifying the local oxygen concentration gradient using dynamic secondary ion mass spectrometry (SIMS) has been made by Rhamdhani and Brooks.[38,39] The results from their investigations suggested the presence of pockets of fluid of the scale 1 to 2 μm with different oxygen contents within the bulk during the reaction. Differences of local oxygen concentration up to 100 and 250 ppm were found near the interface and toward the bulk. Scanning electron microscopy observations of the interface show metal-phase protrusions normal to the interface with a round tip of 1 to 2 μm in diameter.[11] The similarity of the length scale of the protrusions with the scale of the pockets of fluid measured by dynamic SIMS suggests that some pocket of fluid was once at the interface before it moved to the bulk (surface renewal model), and this same pocket of fluid may have caused the oxygen concentration gradient along the interface at the same length scale and may be partly responsible for the formation of the protrusions that may lead to emulsification in microscale.

The effect of oxygen on the surface and interfacial tension are usually described by the adsorption isotherm equation (Eq. [14]), which implies that

$$\frac{d\gamma_{m-s}}{da_O} = -\frac{76424}{1 + 328a_O},\ \text{mNm}^{-1} \qquad [30]$$

or, considering discrete changes,

$$\frac{\Delta\gamma_{m-s}}{\Delta a_O} = \frac{233}{\Delta a_O} \ln\left[\frac{1 + 328\,(a_O^i + \Delta a_O)}{1 + 328\,(a_O^i)}\right],\ \text{mNm}^{-1} \qquad [31]$$

where a_O^i is the initial oxygen activity and Δa_O is the difference in oxygen activity along the interface. The calculated initial oxygen activity at the interface is about 14 ppm (Figure 12). By combining this with the results of Rhamdhani and Brooks, the change of local interfacial tension along the interface due to solutocapillary effect can be estimated. Assuming Henry's law is valid and taking the value of a_O^i = 14 ppm and Δa_O = 100 to 250 ppm, the local decrease of interfacial tension of $\Delta\gamma_{m-s}$ = 274 to 440 mN/m can be obtained. The decrease of interfacial tension of these magnitudes over distances 1 to 2 μm along the interface is significant and may produce more than enough driving flow to induce interfacial instability. Local differences in reaction rate could lead to similar effects due to electrocapillarity and thermocapillarity; however, we have no data to estimate the likely magnitude of such effects.

IV. SUMMARY AND CONCLUSIONS

The solutocapillary, electrocapillary, and thermocapillary effects in the reaction between Fe-Al droplets and CaO-SiO_2-Al_2O_3 slag have been evaluated. The change of the dynamic interfacial tension during reaction is calculated by considering the capillary effects by employing the reaction kinetics and assuming the interfacial tension to be in local equilibrium with the instantaneous interface metal chemistry. The change in interfacial tension calculated from the current approach does not agree well with the results of Riboud and Lucas. However, the current approach has allowed us to compare in a meaningful way the relative effects of electrocapillary, solutocapillary, and thermocapillary on the observed behavior and to draw the following conclusions.

1. The proposed local equilibrium model takes into account all known contributions to the interfacial tension and still does not fully describe the observed phenomenon. This strongly suggests that other forces are at play in the case of reacting interfaces.
2. The electrocapillary effect was found to be dominant in the system studied. It contributed approximately 85 pct of the total magnitude of the maximum interfacial tension depression.
3. Solutocapillarity was found to give a constant effect on interfacial tension with the exception of the first few minutes of reaction. The solutocapillary effect contributed 15 pct of the total magnitude of the maximum interfacial tension depression.
4. The thermocapillary effect on the change of interfacial tension was found to be negligible even with a conservative estimate of the heat dissipation rate.
5. By combining the calculated oxygen activity at the interface from this work with the dynamic SIMS results, the local gradient of interfacial tension along the interface can be estimated, *i.e.*, $\Delta\gamma_{m-s}$ = 274 to 440 mN/m over a 1- to 2-μm distance.

The solutocapillary, thermocapillary, and electrocapillary effects on the dynamic interfacial phenomena in high-temperature reactions are only partially understood. Thus, our conclusions on the dominance of electrocapillary effects are worthy of further research.

ACKNOWLEDGMENTS

M.A. Rhamdhani thanks Mr. G. Bishop, Mr. E. Codispodi, Mr. R. Meguerian, Mr. T. Kaneyasu, Dr. Subagyo, and Dr. F. Ji for their help with the experimental work.

APPENDIX

The following table shows the silicon and aluminum contents in the bulk obtained from experiments and the calculated silicon, aluminum contents, and corresponding local equilibrium oxygen activities during reaction between Fe-4.45 wt pct Al and CaO-SiO_2-Al_2O_3 at 1600 °C up to 10 minutes reaction time.

Time (min)	$S(t)$ (mm^2)	Pct Si_t^{bulk}	Pct Al_t^{bulk}	Pct Si_t^{int}	Pct Al_t^{int}	h_O (ppm)
0	303	0	4.45	1.55	2.27	13.66
5	440	0.74	3.65	2.54	0.71	10.62
10	1261	1.99	2.01	2.39	0.73	11.13

The silicon content at the interface was calculated using Eq. [18].

$$\frac{\left(\text{pct Si}_{t+1}^{\text{bulk}} - \text{pct Si}_{t}^{\text{bulk}}\right)}{t_{t+1} - t} = Z_{Si} \cdot \left(\text{pct Si}_{t}^{\text{int}} - \text{pct Si}_{t}^{\text{bulk}}\right) \quad [A1]$$

For example, at $t = 5$ minutes, the value $k_m^{\text{Si}} = 1.25\ k_m^{\text{Al}} = 1.875 \times 10^{-6}$ m/s = 0.1125 mm/min, $V_m = 357\ \text{mm}^3$, and $S(t) = 440\ \text{mm}^2$. Thus, $Z_{\text{Si}} = k_m^{\text{Si}}\ S(t)/V_m = 0.139\ \text{min}^{-1}$.

$$\frac{1.99 - 0.74}{10 - 5} = 0.25 = 0.139\left(\text{pct Si}_{t}^{\text{int}} - 0.74\right)$$
$$\rightarrow \text{pct Si}_{i}^{\text{int}} = 2.54 \quad [A2]$$

The same calculation was used to calculate silicon content at the interface at different times of reaction. The aluminum contents at the interface during the reaction were also determined using the same method considering Eq. [19].

The local equilibrium oxygen contents were determined using thermodynamic calculations and by considering the calculated concentrations at the interface.

$$(SiO_2) = \underline{Si}_{\text{int}} + 2\underline{O}_{\text{int}} \qquad \log K_{1873} = -4.64^{[25]} \quad [A3]$$

$$K = \frac{h_{\text{Si}} \cdot {h_{\text{O}}}^2}{a_{SiO_2}}$$
$$\log K = \log h_{\text{Si}} + 2 \log h_{\text{O}} - \log a_{SiO_2} \quad [A4]$$

where $h_{\text{Si}} = f_{\text{Si}}$ (wt pct *Si*) and $h_{\text{O}} = f_{\text{O}}$ (wt pct O).

The activity coefficients of components *i*, f_i, were calculated by considering the first- and second-order interaction coefficients as follows:

$$\log f_i = \sum_{j=2}^{n} e_i^j(\text{pct j}) + \sum_{j=2}^{n} {r_i}^j(\text{pct j})^2 + \sum_{j,k=2}^{n} {r_i}^{j,k}(\text{pct j})(\text{pct k}) \quad [A5]$$

where e_i^j, ${r_i}^j$, and ${r_i}^{j,k}$ are the first, second, and cross-product second interaction coefficients. The interaction coefficients used in the calculation were taken from Deo and Boom[25] and Sigworth and Elliott[26]] and are shown in Table II. The cross-product second-order interaction coefficients ${r_i}^{j,k}$ were calculated using reciprocal relationships, as derived by Lupis and Elliott.[27]

Thus, the following equations can be written for silicon and oxygen, respectively:

$$\begin{aligned}\log f_{\text{Si}} &= e_{\text{Si}}^{\text{Si}}(\text{wt pct Si}) + e_{\text{Si}}^{\text{O}}(\text{wt pct O}) + e_{\text{Si}}^{\text{Al}}(\text{wt pct Al}) \\ &+ r_{\text{Si}}^{\text{Si}}(\text{wt pct Si})^2 + r_{\text{Si}}^{\text{O}}(\text{wt pct O})^2 + r_{\text{Si}}^{\text{Al}}(\text{wt pct Al})^2 \\ &+ r_{\text{Si}}^{\text{Si,O}}(\text{wt pct Si})(\text{wt pct O}) + r_{\text{Si}}^{\text{Si,Al}}(\text{wt pct Si})(\text{wt pct Al}) \\ &+ r_{\text{Si}}^{\text{Al, O}}(\text{wt pct Al})(\text{wt pct O}) \\ \log f_{\text{Si}} &= 0.11(\text{wt pct Si}) - 0.23(\text{wt pct O}) \\ &+ 0.058(\text{wt pct Al}) - 0.0021(\text{wt pct Si})^2 \\ &+ 0.00332(\text{wt pct Si})(\text{wt pct O}) \quad [A6]\end{aligned}$$

$$\begin{aligned}\log f_{\text{O}} &= e_{\text{O}}^{\text{O}}(\text{wt pct O}) + e_{\text{O}}^{\text{Si}}(\text{wt pct Si}) + e_{\text{O}}^{\text{Al}}(\text{wt pct Al}) \\ &+ r_{\text{O}}^{\text{O}}(\text{wt pct O})^2 + r_{\text{O}}^{\text{Si}}(\text{wt pct Si})^2 + r_{\text{O}}^{\text{Al}}(\text{wt pct Al})^2 \\ &+ r_{\text{O}}^{\text{O,Si}}(\text{wt pct O})(\text{wt pct Si}) + r_{\text{O}}^{\text{O,Al}}(\text{wt pct O})(\text{wt pct Al}) \\ &+ r_{\text{O}}^{\text{Al,Si}}(\text{wt pct Al})(\text{wt pct Si}) \\ \log f_{\text{O}} &= -0.2(\text{wt pct O}) - 0.131(\text{wt pct Si}) \\ &- 2.81(\text{wt pct Al}) + 1.7(\text{wt pct Al})^2 \\ &- 0.0006(\text{wt pct O})(\text{wt pct Si}) \quad [A7]\end{aligned}$$

Substituting $\log f_{\text{O}}$ and $\log f_{\text{Si}}$ to Eq. [A4], one will obtain

$$\begin{aligned}\log K &= \log(\text{wt pct Si}) - 0.152(\text{wt pct Si}) \\ &- 0.63(\text{wt pct O}) - 5.562(\text{wt pct Al}) \\ &- 0.0021(\text{wt pct Si})^2 + 3.4(\text{wt pct Al}) \\ &+ 0.00212(\text{wt pct Si})(\text{wt pct O}) + 2\log(\text{wt pct O}) \\ &- \log a_{SiO_2} \quad [A8]\end{aligned}$$

By substituting the values

$\log K = -4.64$, $a_{SiO_2} = 0.25$[24], wt pct $Si = 2.54$ and wt pct Al = 0.71

the following is obtained for $t = 5$ minutes:

$$2\log(\text{wt pct O}) - 0.625(\text{wt pct O}) + 3.012 = 0 \quad [A9]$$

Equation [A9] is solved using the Newton–Rhapson method, resulting in

$$\text{O} = 319\ \text{ppm}$$

The oxygen activity is then calculated using

$$\begin{aligned}h_{\text{O}} &= (\text{wt pct O}) \cdot f_{\text{O}} \\ &= (\text{wt pct O}) \\ &\cdot 10^{-0.2(\text{wt pct O}) - 0.131(\text{wt pct Si}) - 2.81(\text{wt pct Al}) + 1.7(\text{wt pct Al})^2 - 0.0006(\text{wt pct O})(\text{wt pct Si})} \\ &= 10.62\ \text{ppm} \quad [A10]\end{aligned}$$

The same calculation was used to calculate local equilibrium oxygen content at different times of reaction.

REFERENCES

1. P. Kozakevitch, G. Urbain, and M. Sage: *Rev. Metall.*, 1955, vol. 2, pp. 161-72.
2. H. Ooi, T. Nozaki, and H. Yoshii: *Trans. Iron Steel Inst. Jpn.*, 1974, vol. 14, pp. 9-16.
3. P.V. Riboud and L.D. Lucas: *Can. Metall. Q.*, 1981, vol. 20 (2), pp. 199-208.
4. A. Sharan and A.W. Cramb: *Metall. Mater. Trans. B*, 1995, vol. 26B, pp. 87-94.
5. Y. Chung and A.W. Cramb: *Phil. Trans. R. Soc. London A*, 1998, vol. 356, pp. 981-93.
6. Y. Chung and A.W. Cramb: *Metall. Mater. Trans. B*, 2000, vol. 31B, pp. 957-71.
7. K. Mukai: *Iron Steel Inst. Jpn. Int.*, 1992, vol. 32 (1), pp. 19-25.
8. A. Jakobsson, M. Nasu, J. Mangwiru, K.C. Mills, and S. Seetharaman: *Phil. Trans. R. Soc. London A*, 1998, vol. 356, pp. 995-1001.
9. R. Parra and M. Allibert: *Can. Metall. Q.*, 1999, vol. 38 (1), pp. 11-21.
10. F.D. Richardson: *Can. Metall. Q.*, 1982, vol. 21 (2), pp. 111-19.
11. M.A. Rhamdhani, K.S. Coley, and G.A. Brooks: *Proc. Int. Symp. on Oxygen in Steelmaking COM 2004*, Aug. 2004, TMSCIM, Hamilton, Canada, 2004, pp. 203-17.
12. M.A. Rhamdhani, G.A. Brooks, and K.S. Coley: *Metall. Mater. Trans. B*, 2005, vol. 36B, pp. 219-27.
13. F. Ji, M.A. Rhamdhani, Subagyo, M. Barati, K.S. Coley, G.A. Brooks, G.A. Irons, and S.A. Nightingale: *High Temp. Mater. Processing*, 2003, vol. 22 (5-6), pp. 359-67.
14. T. Yuge: *J. Heat Transfer, Sec.* C, 1960, vol. 82, pp. 214-38.
15. T. Iida and R.I.L. Guthrie: *The Physical Properties of Liquid Metals*, Oxford University Press, New York, NY, 1988, p. 133.
16. A. Adachi, K. Ogino, and T. Suetaki: *Tetsu-to-Hagané*, 1964, vol. 50, p. 1838.

17. B.V. Szyszkowski: *Z. Phys. Chem*., 1908, vol. 64, pp. 385-414.
18. G.R. Belton: *Metall. Trans. B*, 1976, vol. 7B, pp. 35-42.
19. H. Sun, N. Yoneda, K. Nakashima, and K. Mori: *Proc. 5th Int. Symp. Molten Slags, Fluxes and Salts*, Sydney, 1997, pp. 149-56.
20. H. Gaye, L.D Lucas, M. Olette, and P.V. Riboud: *Can. Metall. Q*., 1984, vol. 23 (2), pp. 179-91.
21. N. Shinozaki, T. Kurashige, K. Mori, and Y. Kawai: *J. Jpn. Inst. Met*., 1982, vol. 46 (1), pp. 60-66.
22. K. Ogino, S. Hara, T. Miwa, and S. Kimoto: *Trans. Iron Steel Inst. Jpn*, 1984, vol. 24, pp. 522-31.
23. Y. Kawai and Y. Shiraishi: *Handbook of Physico-Chemical Properties at High Temperatures*, ISIJ, Tokyo, 1988, pp. 186-8.
24. R.H. Rein and J.H. Chipman: *Trans. TMS-AIME*, 1965, vol. 233, pp. 415-25.
25. B. Deo and R. Boom: *Fundamentals of Steelmaking Metallurgy*, Prentice-Hall International, New York, NY, 1993, pp. 54-55.
26. G.K. Sigworth and J.F. Elliott: *Met. Sci*., 1974, vol. 8, pp. 298-310.
27. C.H.P. Lupis and J.F. Elliott: *Acta Metall*., 1966, vol. 14, pp. 529-38.
28. G. Li and H. Suito: *Metall. Mater. Trans. B*, 1997, vol. 28B, pp. 251-8.
29. G. Li and H. Suito: *Metall. Mater. Trans. B*, 1997, vol. 28B, pp. 259-64.
30. B.V. Patrov: in *Surface Phenomena in Metallurgical Processes*, A.I. Belyaev, ed., Consultants Bureau, New York, NY, 1965, pp. 129-33.
31. I.S. Sinel'shchikova and Y.P. Nikitin: *Izv. Chern. Metall*., 1978, vol. 8, pp. 10-3.
32. A.V. Deev, A.M. Panfilov, S.I. Popel, and N.A. Klinskaya: *Izv. Chern. Metall*., 1980, vol. 9, pp. 16-20.
33. A.A. Deryabin, S.I. Popel, and L.N. Saburov: *Russ. Met. (Metally)*, 1968, No. 5, pp. 37-43.
34. A.A. Deryabin, S.I. Popel, and L.N. Saburov: *Russ. Met. (Metally)*, 1969, No. 1, pp. 50-55.
35. K. Nagata, M. Kawakami, and K.S. Goto: in *Metal-Slag-Gas Reactions and Processes*, Z.A. Foroulis and W.W. Smeltzer, eds., The Electrochemical Society, Inc., Princeton, NJ, 1975, pp. 183-98.
36. A.M. Panfilov: Ph.D. Thesis, Urals Polytechnical Institute, Sverdlovsk (Ekaterinberg), Russia, 1973.
37. M.A. Rhamdhani, G.A. Brooks, and S.A. Nightingale: *Proc. Int. Symp. on Metal/Ceramic Interactions COM 2002*, Aug. 2002, TMSCIM, Montreal, Canada, 2002, pp. 303-13.
38. M.A. Rhamdhani and G.A. Brooks: *Metall. Mater. Trans. B*, 2003, vol. 34B, pp. 355-58.
39. M.A. Rhamdhani and G.A. Brooks: *Proc. 60th Electric Arc Furnace Conf*., ISS, San Antonio, TX, 2002, pp. 787-96.